
Article:
Sinclair, John, Hirohata, Atsufumi orcid.org/0000-0001-9107-2330, Vallejo Fernandez, Gonzalo orcid.org/0000-0002-4826-1547 et al. (2 more authors) (2019) Thermal stability of exchange bias systems based on MnN. Journal of Magnetism and Magnetic Materials. pp. 278-283. ISSN: 0304-8853

https://doi.org/10.1016/j.jmmm.2018.12.018

Thermal Stability of Exchange Bias Systems Based on MnN

J. Sinclair[1], A. Hirohata[2], G. Vallejo-Fernandez[1], M. Meinert[3], and K. O'Grady[1]

[1]Department of Physics, University of York, Heslington, York, YO10 5DD, UK

[2]Department of Electronic Engineering, University of York, Heslington, York, YO10 5DD, UK

[3]Center for Spinelectronic Materials and Devices, Faculty of Physics, Bielefeld University, 33615 Bielefeld, Germany

Email addresses:

J. Sinclair: js946@york.ac.uk

A. Hirohata: atsufumi.hirohata@york.ac.uk

G. Vallejo-Fernandez: gonzalo.vallejofernandez@york.ac.uk (corresponding author)

M. Meinert: meinert@physik.uni-bielefeld.de

K. O'Grady: kevin.ogrady@york.ac.uk

Declarations of interest: none

Abstract

At the present time there is a requirement to identify new antiferromagnetic alloys or compounds which might be suitable for the production of exchange bias systems. The phenomenon of exchange bias remains crucial for the operation of all read heads in hard disk drives and also has potential for use in magnetic random access memory (MRAM) systems. There is also an increasing interest in the use of antiferromagnets themselves in spintronic devices. Generally for applications the alloy IrMn is used, however given that Iridium is one of the rarest, and therefore most expensive elements on Earth, there is a search for alternative materials. In this paper we report on a study of the compound MnN in terms of its thermal stability. We have produced polycrystalline films of this compound with sub 10 nm grains and examined the thermal stability in layers of thicknesses of up to 30 nm. Using thermal activation studies we have determined a room temperature value of the anisotropy constant of this compound in a tetragonal structure of up to $(6.3\pm0.3)\ x10^6$ erg/cm^3. The antiferromagnetic grains can be aligned by thermal annealing at an optimum temperature of 380K. Above this temperature the magnetic properties deteriorate possibly due to nitrogen desorption.

1. Introduction

The phenomenon of exchange bias discovered by Meiklejohn and Bean in 1956 [1] remains crucial for the production of giant magnetoresistance (GMR) and tunnelling magnetoresistance (TMR) devices [2]. In such systems a structure similar to that shown schematically in Figure 1 is used, e.g. in read heads for hard disk drives, where the ferromagnetic (F) layers are typically CoFeB for the bottom layer and CoFe for the upper layer. In TMR devices the inclusion of Boron is to promote the crystallisation of the non-magnetic layer which in general is MgO. The antiferromagnetic (AF) layer in all commercial devices is generally the alloy IrMn. This alloy has a compositional ratio Mn:Ir which lies in the range from the stoichiometric value of 3 but for optimum performance is generally closer to 4 [3]. The seed layers can be a range of materials including NiCr, Cu, Ru or in read head sensors a ferromagnetic alloy of NiFeCr is used which also acts as a shield to prevent crosstalk between bits of information stored on the disk and hence is required to be magnetic.

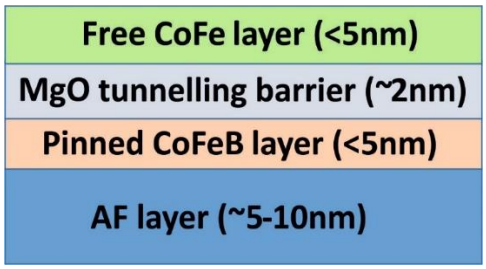

Figure 1. Schematic structure of a TMR junction.

The reasons for the choice of IrMn as the AF material lies in the fact that this alloy is highly corrosion resistant when compared with alternatives such as FeMn, readily crystallises when deposited by magnetron sputtering or ion beam deposition, and has a grain size of around 10 nm which can be easily controlled by the IrMn deposition rate and the choice of seed layer. Furthermore IrMn when deposited in this way crystallises in an fcc phase with the AF spin

ordering lying along the (111) planes. The choice of a seed layer to give close lattice matching between itself and the IrMn allows for texturing of the (111) planes in the plane of the film. However the orientation of the planes within the film will be 2-dimensional (2-D) random. This in-plane texturing leads to a significant increase in the effective anisotropy constant of the IrMn depending on the degree of texture achieved [4].

The element Ir is typically found with deposits of Pt but only at a concentration of 0.1%. Hence not only is the material rare but it is also very expensive and because of its application in spintronic devices is now subject to major price fluctuations due to market speculation. Because of these difficulties a number of alternative materials have been considered as potential AF materials for exchange bias systems [5]. For example a fairly extensive study of Heusler alloys has been undertaken in an attempt to find AF compositions and phases such that the resulting material would be suitable for use in exchange bias systems. One of those alloys, Ru_2MnGe, has been grown in thin film form exhibiting an AF phase and is capable of inducing exchange bias in an Fe layer grown adjacent to it [6]. However the resulting maximum blocking temperature, i.e. the temperature at which the loop shift vanishes after measuring hysteresis loops at elevated temperatures, was found to be $T_B = 130K$. This was the best performing composition that has, as yet, been identified. The majority of Heusler alloys crystallise in a relatively complex cubic structure which indicates that in general they will not have a significant anisotropy unless there is an unusual spin structure such as that in IrMn where the moment bearing ions lie in the (111) planes. To date a Heusler alloy with such a spin structure has not been identified experimentally and such an occurrence may be somewhat improbable as in general, the three atoms composing the Heusler alloy structures are of a similar size as distinct from the case in IrMn where a very large atom is present.

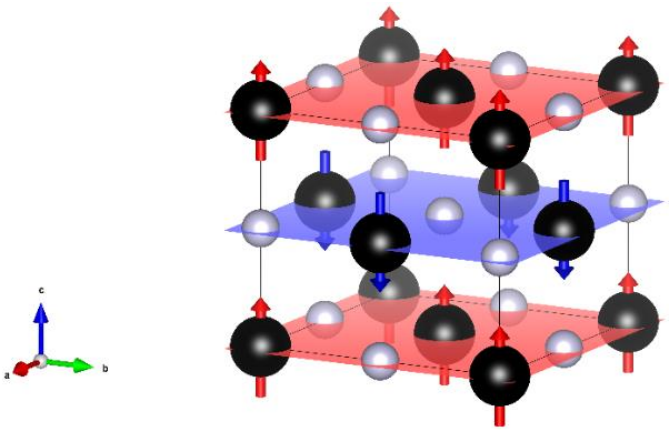

Figure 2. Atomic arrangement in MnN in the tetragonal phase. Larger atoms with an arrow represent Mn atoms while the smaller ones denote N.

An alternative material which is known to have a structure generating a moderate anisotropy is the compound MnN. This material, whose development has been pioneered by Meinert and co-workers [7], can exist in a tetragonal structure which by its very nature creates an anisotropy. The atomic arrangement of the tetragonal phase is shown in Figure 2. Whilst the tetragonal structure is anisotropic, the c/a ratio is relatively modest at 1.04 and in consequence a modest anisotropy is expected. Nonetheless the compound has a relatively high Néel temperature of 655K [8] and so, in principle, can produce an AF material that would be suitable for devices.

Accordingly in this work we have undertaken a study of the anisotropy and thermal stability of MnN with a view to determining the practicality and applicability of MnN for utilisation in GMR and/or TMR stacks.

2. Thermal activation of AF grains

The control and therefore the measurement of the anisotropy of AF layers for devices is crucial for their operation. Our previous work, summarised in Ref. 9, has shown that the

reproducible control of the magnetic and thermal history of a given sample allows for the state of the AF to be inferred at all points from the state of the neighbouring magnetic layer. This is despite the fact that no direct magnetic measurement of the AF grains is possible. After initial deposition, the typical hysteresis loop of an exchange bias system consisting of a seed layer followed by an AF layer of IrMn and an F layer of CoFe is found to be symmetric about the origin but often with an enhanced coercivity due to the anisotropy of the AF layer leading to increased domain wall pinning in the F layer. Subsequently the system can be field annealed in a process referred to as 'setting' the AF. In this process the application of a field serves to saturate the CoFe layer and the exchange field from this F layer then aligns the orientation of the antiferromagnetically coupled spins in the AF layer in the direction of the field. Upon cooling, this leads to a shifted loop. However another unusual phenomenon occurs in that the first loop measured after setting does not reproduce in subsequent measurements on the foregoing branch of the loop. This phenomenon is known as training and has been shown to arise due to the degree of ordering of interface spin clusters some of which are capable of being reversed when the F layer is reversed again due to the reversal in the exchange coupling from the F layer on the AF [10].

The measurement of what is apparently a simple hysteresis loop is further complicated by the effect of the exchange field from the F layer acting on the bulk of the AF grains. In the same way that the setting process takes place, it is possible that once the F layer is reversed the now negative exchange field from the F layer can cause a realignment of the AF grains into the opposite orientation to that originally achieved by setting. This is the case if the grain size is small or the anisotropy of the AF is weak. Hence it is critical that measurements of shifted loops are made at a temperature sufficiently low so that the AF grains are thermally stable. If this is not the case then as the loop is traversed there will occur repeated reversals

and realignment of the AF grains during the field sweep. The existence of such thermal instability can be established by first setting the AF, measuring two loops to remove any training effect and then holding the F layer at negative saturation for a defined period of time, typically 30 minutes, to ensure that a subsequently measured loop reproduces. If this is not the case then the measurement has to be undertaken at progressively lower temperatures until thermal stability is achieved and observed via the reproduction of the loop. The temperature below which no thermal activation occurs we denote T_{NA}.

This thermal instability of AF grains was first observed by Fulcomer and Charap [11] and has subsequently been studied in detail in our previous work [9]. Detailed control of the thermal activation of the reversal of AF grains can provide insight into the overall stability and thereby suitability of any new material and can also allow for the determination of the effective anisotropy constant K_{AF} of the material [12]. Such studies are crucial if alternative AF materials to IrMn are to be developed for applications.

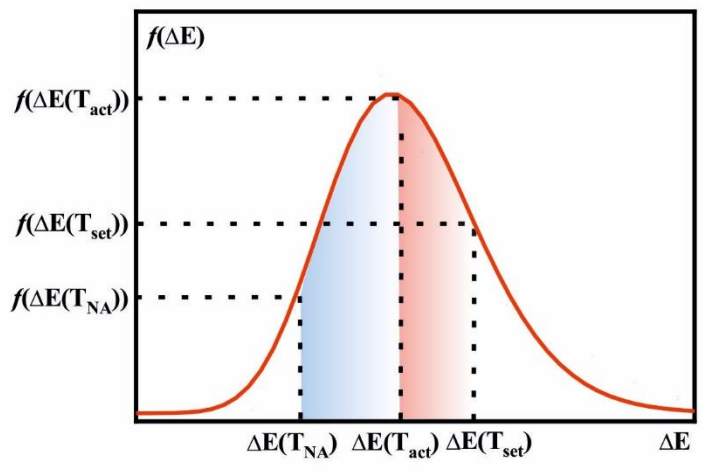

Figure 3. Schematic of the energy barriers to reversal in the MnN layer, showing the fractions of the energy barriers oriented parallel or antiparallel to the original set direction with the shaded areas representing the two integrals in Equation 1.

In order to determine K_{AF}, samples are initially set at a temperature T_{set} for a period of time t_{set}. The samples are then cooled to T_{NA}. A reverse field is then applied to saturate the F layer in the opposite direction used during the setting process. The AF grains are then progressively reversed by raising the temperature to values of T_{act} for a period of time t_{act}. The samples are then cooled back to T_{NA} and the hysteresis loops measured after removing the training effect. By following these steps the AF reversal can be controlled via a change in the value of H_{EX} from negative to positive values and the distribution of blocking temperatures measured. The temperature at which H_{EX} becomes zero is known as the median blocking temperature $<T_B>$. For a given value of T_{act}, H_{EX} is given by:

$$H_{EX}(T_{act}) \propto \int_{\Delta E(T_{act})}^{\Delta E(T_{set})} f(\Delta E)d(\Delta E) - \int_{\Delta E(T_{NA})}^{\Delta E(T_{act})} f(\Delta E)d(\Delta E) \quad (1)$$

where ΔE is the energy barrier to reversal for a given AF grain, $f(\Delta E)$ is the distribution of energy barriers in the AF and ΔE (T_{act}) is the critical energy barrier that determines the fraction of the AF that will reverse at the temperature T_{act} after thermally activating for, in this case, 30 minutes. ΔE (T_{set}) represents the energy barrier of the AF grains that cannot be set at T_{set} due to their anisotropy energy being too large and ΔE (T_{NA}) refers to the fraction of the AF that remains thermally unstable, if any, at the temperature of measurement T_{NA}. In the ideal case where the measurements are done under thermal activation free conditions $\Delta E(T_{NA})$ can be 0. Equation 1 is shown graphically in Figure 3. The distribution of energy barriers to reversal ΔE is directly proportional to the distribution of volumes which can been measured from TEM images [9]. By using the Néel-Arrhenius equation (in zero field) shown below the critical values of the energy barrier can be calculated,

$$\tau^{-1} = f_0 \exp\left(-\frac{K_{AF}(T)V}{kT}\right) \quad (2)$$

where $K_{AF}(T)$ is the anisotropy constant of the material at a given temperature T, V is the volume of a given grain, f_0 is the attempt frequency, k_B is Boltzmann's constant and τ is the

time of measurement. Rearranging Equation 2 it can be shown that for the thermal activation measurements described above:

$$K_{AF}(T)V = ln(f_0 t_{act})k_B T \quad (3)$$

where t_{act} is the time for which thermal activation with the F layer reversed was undertaken. It is important to note that K_{AF} is temperature dependent since its origin is magnetocrystalline and is of the form [12]

$$K_{AF}(T) = K_{AF}(0)\left(1 - \frac{T}{T_N}\right) \quad (4)$$

based on $K_{AF} \propto [m_{AF}(T)/m_{AF}(0)]^3$ and the approximation $m_{AF}(T) \propto (T - T_N)^{1/3}$ [13], where m_{AF} is the moment of one of the AF sublattices.

3. Experimental

To investigate the magnetic properties of MnN, thin film stacks with the structure Ta (10)/MnN (t_{MnN})/$Co_{70}Fe_{30}$ (2)/Ta (2) were grown on thermally oxidised Si substrates using reactive DC magnetron sputtering at room temperature. Thicknesses are given in nm. The system used was a BESTEC 2" co-sputtering system with a working distance of 134.5mm, and base pressure below 10^{-8} mBar. Prior optimisation conducted by Meinert et al. [7] suggested a 50:50 N_2:Ar gas mixture at a process pressure of 2.3×10^{-3} mBar when depositing the MnN films was appropriate. Growth rates were calibrated in-situ using a crystal deposition rate monitor and checked by X-ray reflectivity (XRR) using a Rigaku SmartLab 9 kW diffractometer. The typical deposition rate for MnN was 0.47 $Å s^{-1}$ at a source power of 50W yielding a lattice constant of 4.27 Å. This is larger than the bulk value reported in the literature [14]. No other phases were observed as indicated by the θ/2θ X-ray diffraction (XRD) scan shown in Figure 4a for the 30 nm MnN sample. The mass density was obtained from the reflectivity scan shown in Figure 4b which was measured prior to annealing. Simulation and fitting of the reflectivity data yielded a MnN layer thickness of (29.4±0.1) nm

and a density of (6.17±0.08) gcm^{-3}. As can be seen from Figure 4b) there is an initial drop in intensity at ~0.1° with the intensity rising to 100% of the initial intensity at ~0.6°. This was due to the sample geometry as the physical footprint of the beam was of a similar size as the substrate. When fitting, layer thicknesses were obtained from the Fourier transform of the XRR data before refining along with density and surface roughness values. The roughness values obtained were between 0.1 and 0.4 nm. The mass density obtained is significantly larger than the expected value for the stoichiometric θ-MnN AF phase given by Suzuki et al. as 6.03 g/cm^3 [15]. This indicates a contraction in the in-plane lattice constants compared to the literature values.

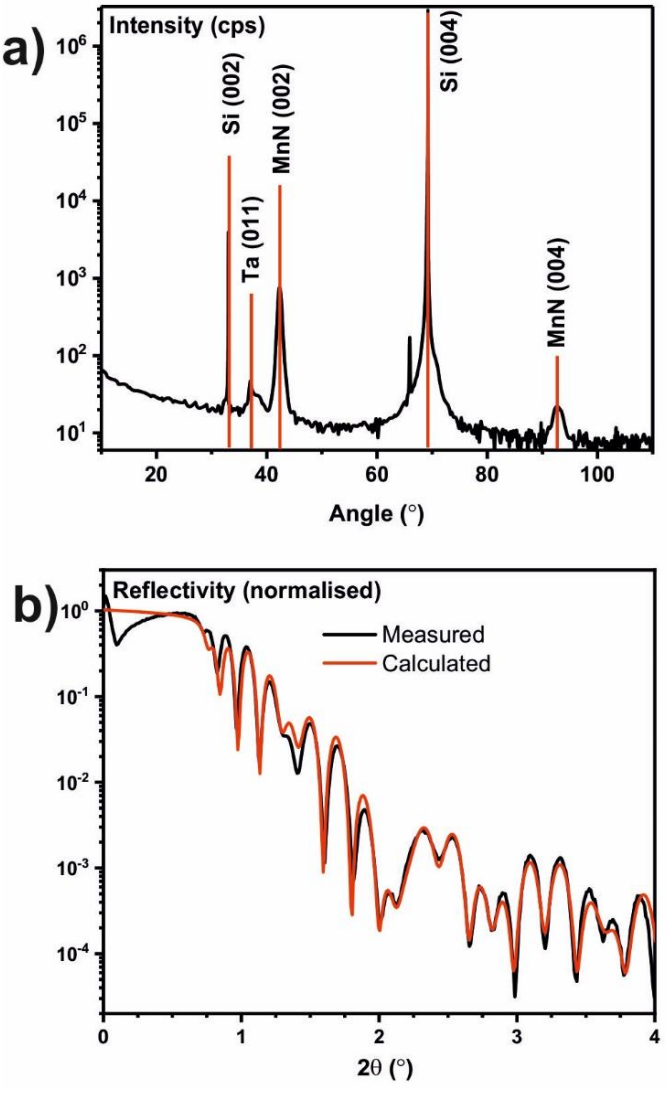

Figure 4. a) θ/2θ scan and b) XRR scan for the 30 nm MnN sample.

An FEI dual beam focused ion beam (FIB) was used for the preparation of a plan view transmission electron microscope (TEM) specimen. Figure 5 shows the grain size distribution and a typical TEM image (inset) for the sample with a 30 nm MnN layer. 750 grains were measured using a Zeiss particle size analyser. To allow for a clear definition of the grains only those meeting the Bragg condition, i.e. showing as black in a bright field image, were measured. As expected for a sputtered thin film the grain size distribution was found to be lognormal with D_m = 4.8 nm and σ = 0.33, where D_m is the median grain size and σ is the standard deviation of ln(D). This value is rather small considering the thickness of the films and is a critical factor in relation to the thermal stability of the film. For instance, assuming a constant thickness, the thermal stability of a 4.8 nm grain is almost 80% smaller than that of a 10nm grain.

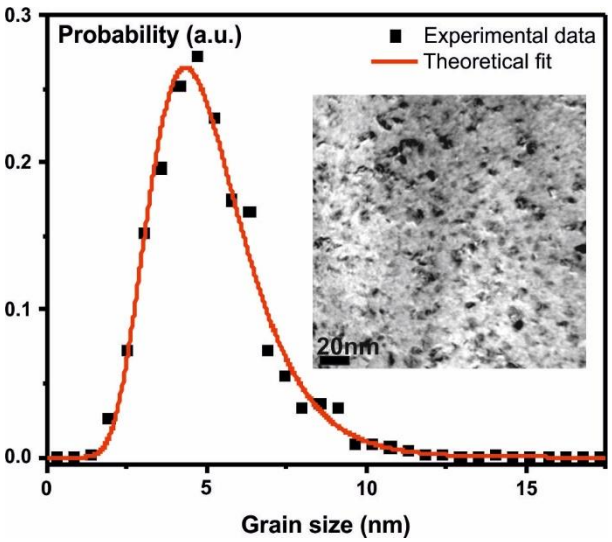

Figure 5. Grain size distribution and TEM image (inset) for the sample with a 30 nm MnN AF layer.

A Microsense model 10 VSM with a continuous flow cryostat enabling temperature control to better than 0.5K/hour was used for the magnetic characterisation of the films. To investigate the thermal stability and exchange bias phenomena present the measurement protocols described in Ref. 9 and summarised in Section 2 were used.

4. Results

As the initial state of the AF is unknown, the first requirement is to set the AF in a reproducible manner. Ideally this would be achieved by field cooling from above the Néel temperature (T_N=(655±3)K [8]). However this could result in interfacial mixing as well as nitrogen desorption. For this reason it is necessary to set at a lower temperature which is possible due to the distribution of thermal activation energies present in a granular system but requires experimental determination of the setting temperature T_{set} and setting time t_{set}. Similarly it is necessary to ensure that no unwanted thermal activation occurs. This is achieved by cooling to a temperature where no thermal activation occurs (T_{NA}). This temperature was determined by trial and error by first setting the sample, then reducing the temperature until the sample could be held with the F layer reversed for 30 min with no change in the exchange bias observed after removal of the training effect. For the 30 nm MnN film, 200K proved sufficiently cold to prevent any thermal activation. Hence all measurements were carried out at that temperature.

Figure 6(a) shows a selection of hysteresis loops obtained for a 30 nm MnN film during setting. These loops show both a shift in both squareness and exchange bias (H_{EX}) as a function of the setting temperature. The first of these effects can be explained by considering the reversal process dominant in the film stack. Normally a thin CoFe layer would exhibit very sharp reversal, dominated by nucleation and rapid domain wall motion. This is clearly not the case for the hysteresis loops obtained at setting temperatures below 375K. The gradual reversal observed is explained by the rotation of domains in the strongly exchanged coupled grains coupled to the randomly orientated MnN layer. The gradual nature of the subsequent reversal indicates a wide distribution of domain wall pinning strengths originating in the MnN. Figure 6(b) shows the exchange bias obtained after each setting temperature

showing an increase in the proportion of the AF set up to ~375K and a sharp decrease in the observed exchange bias after setting above 400K. This decrease is possibly due to desorption of nitrogen from the MnN [16] or an irreversible structural/magnetic transition in the MnN or at the MnN/CoFe interface [7]. The shape of the hysteresis loops as well as the magnitude of the loop shift are in good agreement with recent theoretical investigations by Simon et al. [17], albeit for a different ferromagnetic system. As can be seen in Figure 2 the Mn spins in the MnN layer are oriented out-of-plane. At the interface between the F and AF layers there is ferromagnetic coupling with the spins preferring to lie in a direction parallel to the plane of the interface. This leads to a twisted spin structure across the interface [17].

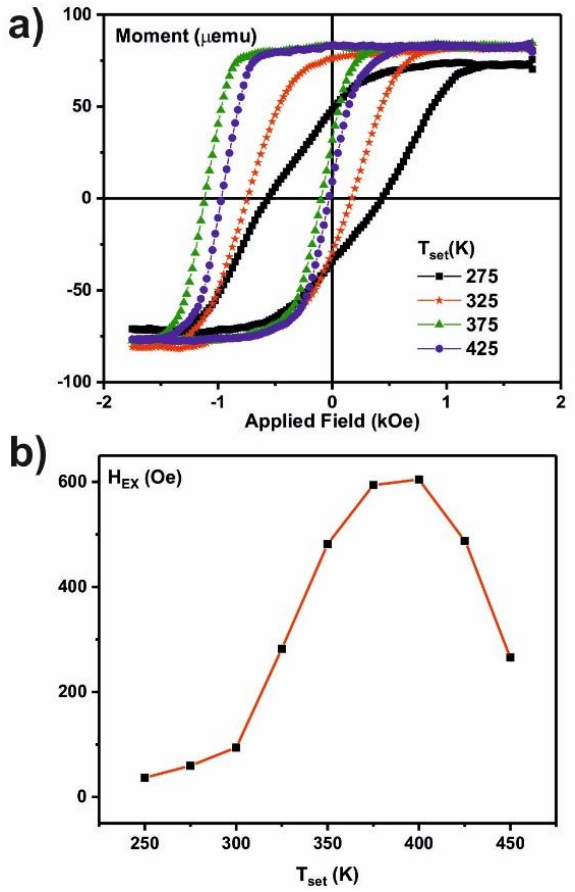

Figure 6. Determination of optimal setting temperature for 30 nm MnN (a) Representative hysteresis loops after setting for 90min at T_{set}, all measurements at 200K. (b) Exchange bias as a function of setting temperature.

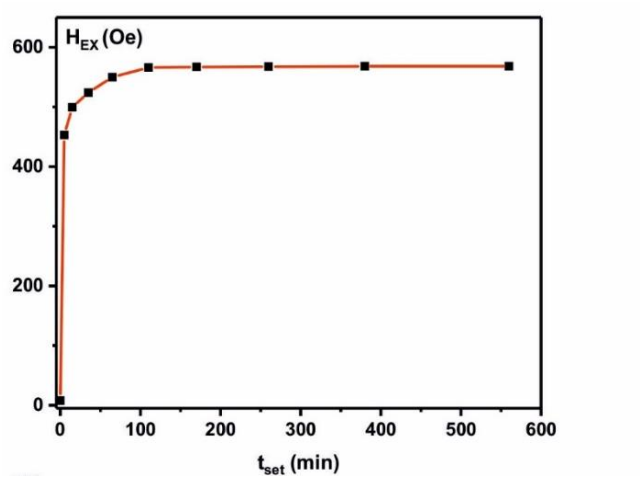

Figure 7. Exploration of the dependence of H_{EX} on t_{set} for the 30 nm MnN sample up to a setting time of 10 hr. All measurements made at 200K.

To determine the necessary setting time an un-set, i.e. as-deposited, MnN sample was set for incrementally increasing times at T_{set} = 380K. Figure 7 shows the values of H_{EX} obtained as a function of the setting time. Each measurement was performed at 200K after removal of any training effect. Over 99% of the maximum exchange bias is observed after t_{set}=110 mins. This setting time was used for the thermal activation measurements described below. No decrease in the value of H_{EX} was observed even after setting for 10 hours which suggests the samples are stable at 380K.

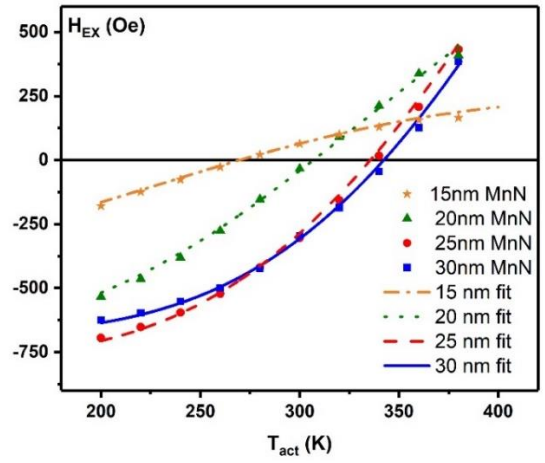

Figure 8. Blocking temperature curves and calculated fits using Equation 1 for the samples studied in this work.

Figure 8 shows the blocking temperature curves for the samples studied in this work. The lines in this figure are calculated fits using Equation 1. The samples were originally set at 380K for 110 minutes based on the data shown in Figs. 6 and 7 in a field of +20 kOe. The samples were then cooled to T_{NA} = 200K. In this case, steps of 20K in T_{act} were used. The fitting parameters used to obtain the fits in Figure 8 are as follows: $f_0 = 2.1 \times 10^{12}$ s^{-1} [18], T_{NA} = 200K, T_N = 655K, T_{set} = 380K, D_m = 4.8nm, σ = 0.33, t_{act} = 1800s and t_{set} = 6600s. Grain volumes were calculated from the measured lateral grain diameter distribution in the films and the thickness of the layer using a cylindrical approximation.

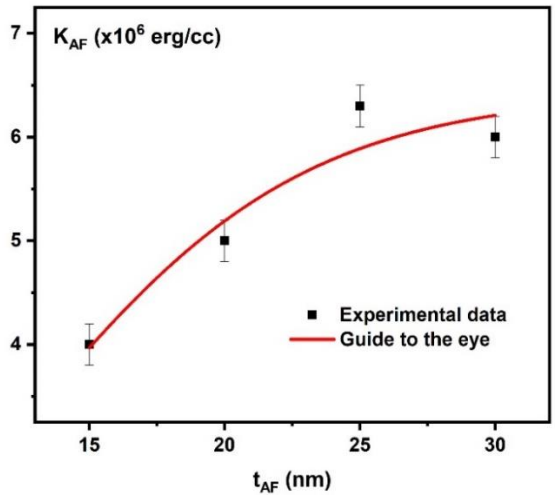

Figure 9. Anisotropy constant at room temperature as a function of the MnN layer thickness.

The value of the anisotropy constant varied from sample to sample which is shown in the data in Figure 8 due to the proportionality of $\langle T_B \rangle$, i.e. the temperature at which $H_{ex} = 0$, to the value of K_{AF} at constant volume. The data is gathered in Figure 9. All samples studied in this work are thick (>10 nm) and a constant value of K_{AF} would be expected across samples [12]. From the data in Figure 9 it is clear that there is a significant variation in the K_{AF} with film thickness. Previous cross section TEM studies on samples grown in Bielefeld showed that the grain growth is columnar so the grain size in each film will be the same for film

thicknesses above a few nanometres. Hence, following Equation 3, the variation in the median value of the blocking temperature $<T_B>$ should vary linearly with t_{AF} as the lateral grain size should be constant. The data in Figure 9 indicates a monotonic increase in K_{AF} with film thickness until a thickness of 25nm is reached. However as only 2 films thicker than this value were measured this result may not be definitive.

The origin of the lower value of K_{AF} in films thinner than 25nm can have two origins. Either the crystal structure may not be the anisotropic tetragonal phase with a c/a ratio of 1.04 or the stoichiometry of the grains may vary with film thickness. To determine which of these parameters is affected we have undertaken a detailed high resolution X-ray diffraction study of the films. The key data from the XRD analysis is shown in Table 1. From this data it is clear that the interplanar spacing is constant within error across films of all thicknesses. Furthermore the c/a ratio is similarly constant within error and the data also confirms that the grain size determined from Scherrer broadening is also constant within error, (8.8±0.2) nm. This data then clearly shows that the origin of the lower anisotropy in the thinner films must lie in the stoichiometry of the grains.

Table 1. Summary of calculated lattice parameters and tetragonal distortion ratios for MnN prepared using magnetron sputtering.

Thickness (nm)	Out of plane (002) (Å)	Out of plane (004) (Å)	In-Plane (200) (Å)	Tetragonal Distortion
15	4.267	4.263	4.077	1.047
20	4.265	4.264	4.107	1.038
25	4.266	4.267	4.078	1.046
30	4.265	4.264	4.114	1.037
Mean	4.266 ± 0.001	4.265 ± 0.002	4.09 ± 0.02	1.042 ± 0.005

It is well known that nitrogen desorption from transition metal nitride compounds can occur but it is somewhat surprising that the effects can be so dramatic. Of course we do not have

direct evidence for the nitrogen content in the films and indeed this is difficult to determine quantitatively. However for the potential application of MnN films of thickness 30nm would be somewhat impractical and ideally layers thinner than 10nm would be used. This may be achievable while maintaining the anisotropy by growth of the films with different levels of the ratio of N_2:Ar in the sputter gas. However other minor changes in the composition of the compound may also increase the stability of the nitrogen component at close to the stoichiometric level.

5. Conclusions

The value obtained for the anisotropy constant for MnN is comparable to that of IrMn (0.6-2.9x10^7 erg/cm^3 [4]), the alloy currently used in all GMR/TMR applications. However, thicknesses >20 nm appear to be necessary to achieve thermal stability above room temperature due to the small grain sizes (D_m ~ 5nm). A possible solution to this problem would be to grow samples with larger lateral grain sizes. This could potentially allow for the reduction in the AF thickness even if the anisotropy is reduced for thinner films. Doping of MnN with elements that could stretch the crystal lattice along the long axis of the unit cell could also help circumvent the problem of the reduction in the anisotropy. Overall, MnN shows some potential as a novel AF material for the replacement of IrMn in device applications.

Acknowledgements

The authors would like to thank Dr. Stephen McVitie from the University of Glasgow for valuable help with TEM sample preparation. This work was part-funded through a project, HARFIR (Heusler Alloy Replacement For Iridium), by the European Commission under the 7th Framework Programme (FP7-NMP-2013-EU-Japan, Grant Agreement No. NMP3-SL-

2013-604398). AH, GVF and KOG also acknowledge financial support from the UK EPSRC (EP/M02458X/1).

References

[1] W. H. Meiklejohn and C.P. Bean, Phys. Rev. **102**, 1413 (1956).

[2] S. M. Thompson, J. Phys. D: Appl. Phys. **41**, 093001 (2008)

[3] N. P. Aley and K. O'Grady, J. Appl. Phys. **109**, 07D719 (2011).

[4] N. P. Aley, G. Vallejo-Fernandez, R. Kroeger, B. Lafferty, J. Agnew, Y. Lu, and K. O'Grady, IEEE Trans. Mag. **44**, 2820 (2008).

[5] A. Hirohata, T. Huminiuc, J. Sinclair, H. Wu, M. Samiepour, G. Vallejo-Fernandez, K. O'Grady, J. Balluf, M. Meinert, G. Reiss, E. Simon, S. Khmelevskyi, L. Szunyogh, R. Yanes Diaz, U. Nowak, T. Tsuchiya, T. Sugiyama, T. Kubota, K. Takanashi, N. Inami, and K. Ono, J. Phys. D: Appl. Phys. **50**, 443001 (2017).

[6] J. Baluff, M. Meinert, J.M. Schmalhorst, G. Reiss, and E. Arenholz, J. Appl. Phys. **118**, 243907 (2015).

[7] M. Meinert, B. Büker, D. Graulich, and M. Dunz, Phys. Rev. B **92**, 144408 (2015).

[8] M. Tabuchi, M. Takahashi, and F. Kanamaru. J. Alloys Comp. **210**, 143 (1994).

[9] K. O'Grady, L.E. Fernandez-Outon, and G. Vallejo-Fernandez, J. Magn. Magn. Mater. **322**, 883 (2010).

[10] B. Kaeswurm and K. O'Grady, J. Appl. Phys. **107**, 09D727 (2010).

[11] E. Fulcomer and S.H. Charap, J. Appl. Phys. **43**, 4190 (1978).

[12] G. Vallejo-Fernandez, L. E. Fernandez-Outon, and K. O'Grady, Appl. Phys. Lett. **91**, 212503 (2007).

[13] M. D. Stiles and R. D. McMichael, Phys. Rev. B **60**, 12950 (1999).

[14] H. Yang, H. Al-Brithen, E. Trifan, D. C. Ingram, and A. R. Smith, J. Appl. Phys. **91**, 1053 (2002).

[15] K. Suzuki, T. Kaneko, H. Yoshida, Y. Obi, H. Fujimori, and H. Morita, J. Alloys Comp. **306**, 66 (2000).

[16] J.-G. Choi, H. J. Lee, and L. T. Thompson, Appl. Surf. Sci. **78**, 299 (1994).

[17] E. Simon, R. Yanes, S. Khmelevskyi, K. Palotás, L. Szunyogh, and U. Nowak, Phys. Rev. B **98**, 094415 (2018).

[18] G. Vallejo-Fernandez, N. P. Aley, J. N. Chapman, and K. O'Grady, Appl. Phys. Lett. **97**, 222505 (2010).